

**Magnetic imaging of layer-by-layer reversal in Co/Pt multilayers with perpendicular anisotropy**

M. Robinson, Y. Au, J. W. Knepper, F. Y. Yang, and R. Sooryakumar

*Department of Physics, The Ohio State University, 191 W. Woodruff Avenue, Columbus, Ohio 43210, USA*

(Received 29 December 2005; revised manuscript received 24 April 2006; published 15 June 2006)

For very thin Co layers, the exchange coupling between adjacent Co layers in Co/Pt multilayers is ferromagnetic and the coupling strength varies nonmonotonically as the nonmagnetic Pt layer thickness ( $t_{\text{Pt}}$ ) ranges from 3 to 75 Å. We report on the magnetization reversal process in a series of  $[\text{Co}(4 \text{ Å})/\text{Pt}(t_{\text{Pt}})]_N$  multilayers observed by magneto-optical Kerr microscopy as a function of  $t_{\text{Pt}}$  and layer repetition  $N$ . The images reveal the evolution of magnetic reversal processes that strongly depend on  $t_{\text{Pt}}$  and therefore on the interlayer coupling. For Co/Pt multilayers with small  $t_{\text{Pt}}$ , e.g., 11 Å, where the Co layers are strongly coupled, the whole multilayer switches as a single ferromagnet. As Co layers are separated farther and become weakly coupled, e.g., at  $t_{\text{Pt}} = 41 \text{ Å}$ , layer-by-layer magnetic reversal is observed. The Kerr images reveal metastable magnetic domain configurations during layer-by-layer switching which is not evident in the measured hysteresis loops during the abrupt magnetic reversal for Co/Pt multilayers with weak interlayer coupling at large  $t_{\text{Pt}}$ .

DOI: [10.1103/PhysRevB.73.224422](https://doi.org/10.1103/PhysRevB.73.224422)

PACS number(s): 75.60.Ch, 75.60.-d, 75.30.Gw, 75.70.Cn

**I. INTRODUCTION**

With rapid advances taking place in the magnetic recording industry, understanding magnetization reversal processes, including the formation and evolution of magnetic domains, have emerged as important issues in data storage and sensor technology. As current magnetic storage density is pushed toward the superparamagnetic limit, it is believed that higher areal densities can be achieved by means of perpendicular recording due to the lower superparamagnetic limit and larger anisotropy in magnetic media with perpendicular anisotropy.<sup>1</sup> Because there are many competing energies involved in the magnetic switching processes, the formation and evolution of magnetic domains during magnetization reversal can be complex and fundamentally interesting.

The impressive progress in data storage science and development over the past two decades has been driven, in part, by discoveries of oscillatory interlayer coupling in ferromagnetic and nonmagnetic multilayers and the occurrence of giant magnetoresistance.<sup>2,3</sup> While most systems that exhibit oscillatory interlayer coupling have in-plane magnetic anisotropy, in recent years multilayers consisting of Co/Pd, Co/Pt structures have attracted attention due to their perpendicular magnetic anisotropy and thus the potential for ultrahigh density data recording applications.<sup>4-7</sup> For instance, investigations have shown that the Co/Pt multilayer structures with perpendicular anisotropy exhibit Ruderman-Kittel-Kasuya-Yosida (RKKY) oscillatory interlayer coupling with a ferromagnetic background between adjacent Co layer as the NM layer thickness increases.<sup>8,9</sup> The overall magnetization reversal properties of such multilayer structures would thus be influenced by the interlayer coupling and the response of the individual Co layers to the applied magnetic field.

In this study, microscopic Kerr imaging was used to study the perpendicular magnetization reversal of Co/Pt multilayers and their dependence on the strength and nature of the interlayer coupling between neighboring Co layers. Unlike conventional magnetometry, such as superconducting quantum interference devices and vibrating sample magnetome-

ters (VSM), that reveal the overall magnetic response of the structure to an external magnetic field, Kerr imaging has, as illustrated in this study, the advantage of yielding the response of individual Co layers with high spatial resolution.

**II. EXPERIMENTAL DETAILS**

Several series of  $[\text{Co}(4 \text{ Å})/\text{Pt}(t_{\text{Pt}})]_N$  multilayers with repetition  $N$  from 5 to 30 were fabricated using a ultrahigh vacuum magnetron sputtering system as described elsewhere.<sup>8</sup> 50 mm long Si wafers with a native oxide layer were used as substrates. A 100 Å Pt buffer layer was first deposited on each wafer, followed by the deposition of Co/Pt multilayers. The Co layers are uniform with a thickness of 4 Å and the Pt layers are wedges with thickness  $t_{\text{Pt}}$  ranging from 0 to 80 Å. Finally, a 30 Å Pt layer was deposited on top as the capping layer to prevent oxidation. Each Si wafer was cut into 40 pieces of 1.25 mm wide strips. Each strip has a thickness variation of 2 Å and  $t_{\text{Pt}}$  refers to the average thickness of the strip. Hysteresis loops were measured with a magnetic field ( $H$ ) perpendicular to the film plane using a LakeShore VSM. As evidenced by hysteresis loops in our previous report, perpendicular anisotropy was observed in all  $[\text{Co}(4 \text{ Å})/\text{Pt}(t_{\text{Pt}})]_N$  multilayers.<sup>8</sup> In this article, Co/Pt multilayers with  $N=5, 8, \text{ and } 12$ , and  $11 \text{ Å} \leq t_{\text{Pt}} \leq 41 \text{ Å}$  were studied using magneto-optical Kerr imaging to reveal the details of magnetic domain-wall formation and propagation during magnetic switching processes.

*In-situ* magneto-optical images based on the polar Kerr effect were recorded at room temperature using 488 nm laser illumination, polarizing the optics and magnetic coils capable of producing magnetic fields perpendicular to the sample surface.<sup>10</sup> The evolution of domain patterns and the reversal of magnetization in the multilayers were mapped through the following sequence. A magnetic field far exceeding the coercive field was initially applied for 3 s to magnetically saturate the sample. Then, the field was reduced to zero. The resulting magnetic state—the initial configuration—appears as a bright Kerr image with *up* magnetization in Figs. 1(c), 2(c), 3(c), and 4(c). The sample is

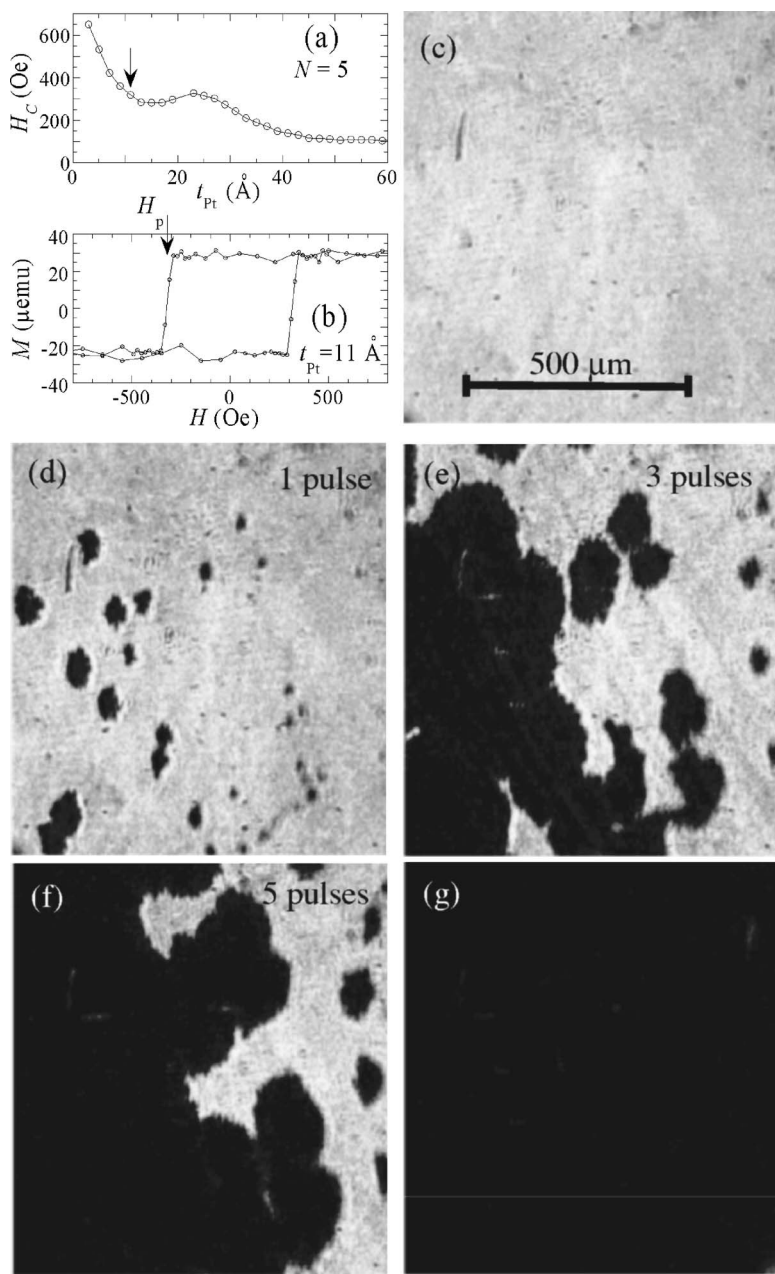


FIG. 1. (a) Room-temperature coercivity ( $H_C$ ) for  $[\text{Co}(4 \text{ \AA})/\text{Pt}(t_{\text{Pt}})]_N$  multilayers with repetition  $N=5$ . (b) Hysteresis loop for sample with  $N=5$ ,  $t_{\text{Pt}}=11 \text{ \AA}$  as indicated by the arrow in (a). (c)–(f) Kerr microscopy images of  $[\text{Co}(4 \text{ \AA})/\text{Pt}(11 \text{ \AA})]_5$  multilayer recorded between repetitive field pulses at  $H_p$  indicated in (b) created by current pulses. The number in each figure corresponds to the number of pulses associated with the image. (g) Kerr image of  $[\text{Co}(4 \text{ \AA})/\text{Pt}(11 \text{ \AA})]_5$  multilayer after saturated by a large magnetic field applied opposite to the initial magnetization.

then subject to a succession of pulsed magnetic fields ( $H_p$ ) each with the same strength close to the coercive value and oriented opposite to the direction of saturate magnetization of the initial configuration, as indicated by the arrows in Figs. 1(b), 2(b), 3(b), and 4(b). This reversal field was created by a 30 ms square current pulse flowing through the magnetic coils. A progression of Kerr images of the magnetic domains was sequentially recorded between repetitive field pulses. The recording time for each Kerr image was 3 s in order to obtain good signal-to-noise ratio. Eventually, a large magnetic field was applied to fully reverse the magnetization.

### III. RESULTS AND DISCUSSION

Figure 1(a) shows the room temperature coercivity,  $H_C$ , for the  $N=5$  multilayer structure  $[\text{Co}(4 \text{ \AA})/\text{Pt}(t_{\text{Pt}})]_5$  as a

function of  $t_{\text{Pt}}$  lying between 3 and 60 Å. A clear peak in  $H_C$  is evident at  $t_{\text{Pt}} \approx 23 \text{ \AA}$ , and the nonmonotonic behavior in  $H_C$  has previously been associated with the interlayer coupling between Co layers through the Pt.<sup>8</sup> Moritz *et al.*<sup>9</sup> have attributed the oscillatory interlayer coupling to RKKY interaction using exchange bias field in Co/Pt multilayer stacks.<sup>9</sup> The arrow in Fig. 1(a) identifies the Pt layer thickness (11 Å) for the particular sample where the reversal was studied using Kerr imaging. The corresponding hysteresis loop of the sample is shown in Fig. 1(b), where the arrow indicates the magnitude of the pulse field  $H_p$  for the magnetization reversal studies. The interlayer coupling which involves both the exchange interaction and dipole interaction between Co layers is always ferromagnetic for the whole range of Pt thickness. While at  $t_{\text{Pt}}=11 \text{ \AA}$ , the coupling strength is strong, the interlayer coupling becomes weaker at larger  $t_{\text{Pt}}$ . Figures 1(c)–1(f) provide some images of the magnetic domain pat-

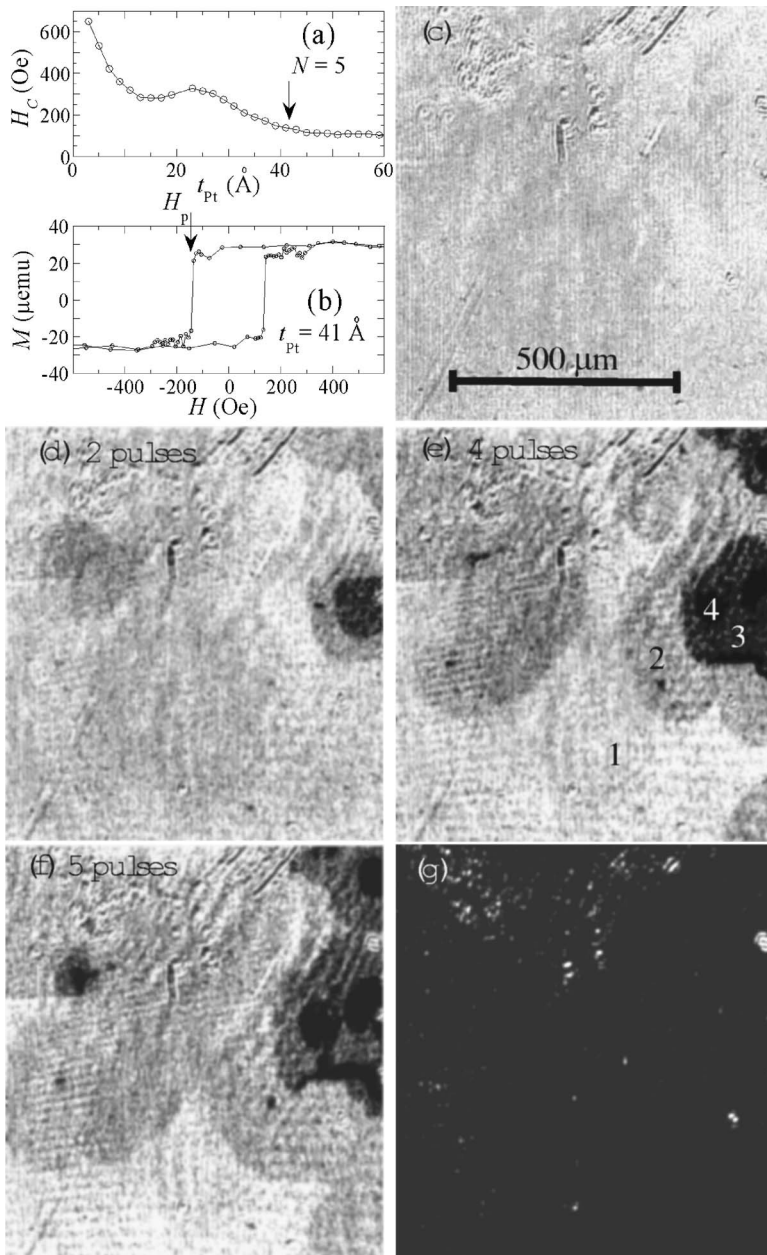


FIG. 2. (a) Room-temperature coercivity for  $[\text{Co}(4 \text{ \AA})/\text{Pt}(t_{\text{Pt}})]_N$  multilayers with repetition  $N=5$ . (b) Hysteresis loop for sample with  $N=5$ ,  $t_{\text{Pt}}=41 \text{ \AA}$ . (c)–(f) Kerr microscopy images of  $[\text{Co}(4 \text{ \AA})/\text{Pt}(41 \text{ \AA})]_5$  multilayer recorded between repetitive field pulses at  $H_p$  indicated in (b). The corresponding number of field pulses is indicated in each image. (g) Kerr image of  $[\text{Co}(4 \text{ \AA})/\text{Pt}(41 \text{ \AA})]_5$  multilayer after saturated opposite to the initial magnetization.

terns in time order during the application of repetitive pulse field  $H_p$ . The numbers in Figs. 1(d)–1(f) indicate the number of pulses associated with each figure. Eventually, a large magnetic field was applied opposite to the initial magnetization to saturate the whole sample with *down* magnetization as shown in Fig. 1(g). A clear evolution from the fully saturated (bright) state with a single domain of *up* magnetization [Fig. 1(c)] to the fully reversed (dark) state of a single *down* domain [Fig. 1(g)] is observed. One observes, in Figs. 1(d)–1(f), the nucleation of the reversed magnetic domains (dark) with *down* magnetization. The *down* domains grow steadily at the expense of the *up* domain by displacing the domain boundaries and nucleating new reversed cells. While a domain wall between an *up* and a *down* domain can move—thereby allowing one domain to grow and the other to shrink, defects and inhomogeneities within the multilayers can serve as pinning sites which freeze the domain wall. The

domain wall will eventually be unpinned when the net gain of Zeeman energy due to the growing of the opposite domains overcomes the domain-wall pinning energy.<sup>11</sup> We note that the images in Fig. 1 show only two distinct contrasts—bright and dark—i.e., the original saturated state with *up* magnetization and the reversed magnetic state with *down* magnetization. Given that the total thickness ( $105 \text{ \AA}$ ) of the  $[\text{Co}(4 \text{ \AA})/\text{Pt}(11 \text{ \AA})]_5$  multilayer plus Pt cap layer is smaller than the skin depth of the probe laser beam (estimated to be  $140 \text{ \AA}$ ),<sup>12</sup> it follows that in this case all five Co layers within a given spatial area switch at the same time. As the reversed magnetization is nucleated at a specific region of a given layer, the strong interlayer coupling, which include the RKKY-type interaction and dipole interaction, ensures that the layers above and below within the same region also reverse. The same behavior of the magnetic switching was observed for the same series of multilayers ( $N=5$ ) with  $t_{\text{Pt}}$



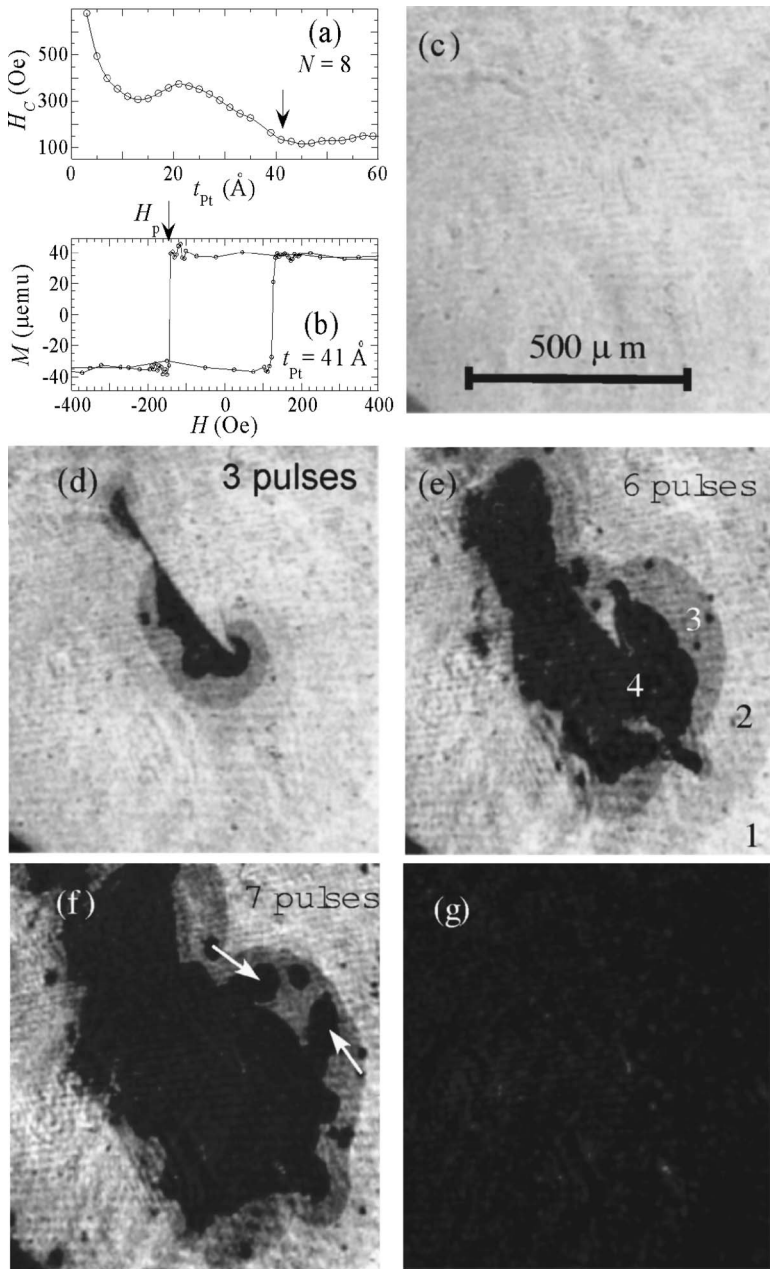


FIG. 3. (a) Room-temperature coercivity for  $[Co(4 \text{ Å})/Pt(t_{Pt})]_N$  multilayers with repetition  $N = 8$ . (b) Hysteresis loop for sample with  $N=8$ ,  $t_{Pt}=41 \text{ Å}$ . (c)–(f) Kerr microscopy images of  $[Co(4 \text{ Å})/Pt(41 \text{ Å})]_8$  multilayer recorded between repetitive field pulses at  $H_p$  indicated in (b). The corresponding number of field pulses is indicated in each image. The white arrows in (f) indicate the two peninsular-shaped regions in Domain 4. (g) Kerr image of  $[Co(4 \text{ Å})/Pt(41 \text{ Å})]_8$  multilayer after saturated opposite to the initial magnetization.

$=21 \text{ Å}$ , where the Co layers are still strongly coupled and the structure reverses as a single ferromagnetic unit.

This observation is in contrast to the domain patterns during magnetization reversal from a multilayer sample with the same number of Co layers ( $N=5$ ), but a greater separation ( $t_{Pt}$ ). At large  $t_{Pt}$ , both the exchange interaction and dipole interaction decreases.<sup>13–15</sup> Figure 2 shows the evolution of the domain patterns from the structure  $[Co(4 \text{ Å})/Pt(41 \text{ Å})]_5$ . As in Fig. 1, ferromagnetic interlayer coupling is corroborated from Fig. 2(a). Due to the greater value of  $t_{Pt}$ , a weaker interlayer coupling than that in the  $t_{Pt}=11 \text{ Å}$  sample (Fig. 1(b)) is suggested from Fig. 2(b) with a smaller  $H_C$ . In these weakly coupled layers, the Kerr images show that the entire structure does not switch as a single ferromagnet but rather the Co layers reverse separately. As field pulses were applied at  $H_p$  indicated in Fig. 2(b), four distinct domains (labeled

1–4) with clearly distinguishable shades are observed [Fig. 2(e)] in this multilayer. A large magnetic field applied opposite to the initial magnetization ultimately aligns all magnetic domains and there is no contrast between them [Fig. 2(g)]. Although the hysteresis loop in Fig. 2(b) shows a sharp magnetic switching which suggests that all the Co layers reverse at the same magnetic field, as discussed below, Kerr images reveal that the Co layers switch separately. The magnetization of a region within a Co layer with the lowest coercivity begins to reverse first [dark regions Fig. 2(d)] and forms a *down* domain. This is followed by a layer-by-layer reversal as is evident from the distinctively different shades of gray in Figs. 2(d)–2(f), when more field pulses cause regions with a little higher coercivity to reverse. Ultimately, except for a few defective inclusions on the surface, a fully dark region develops in Fig. 2(g), when negative saturation of the entire

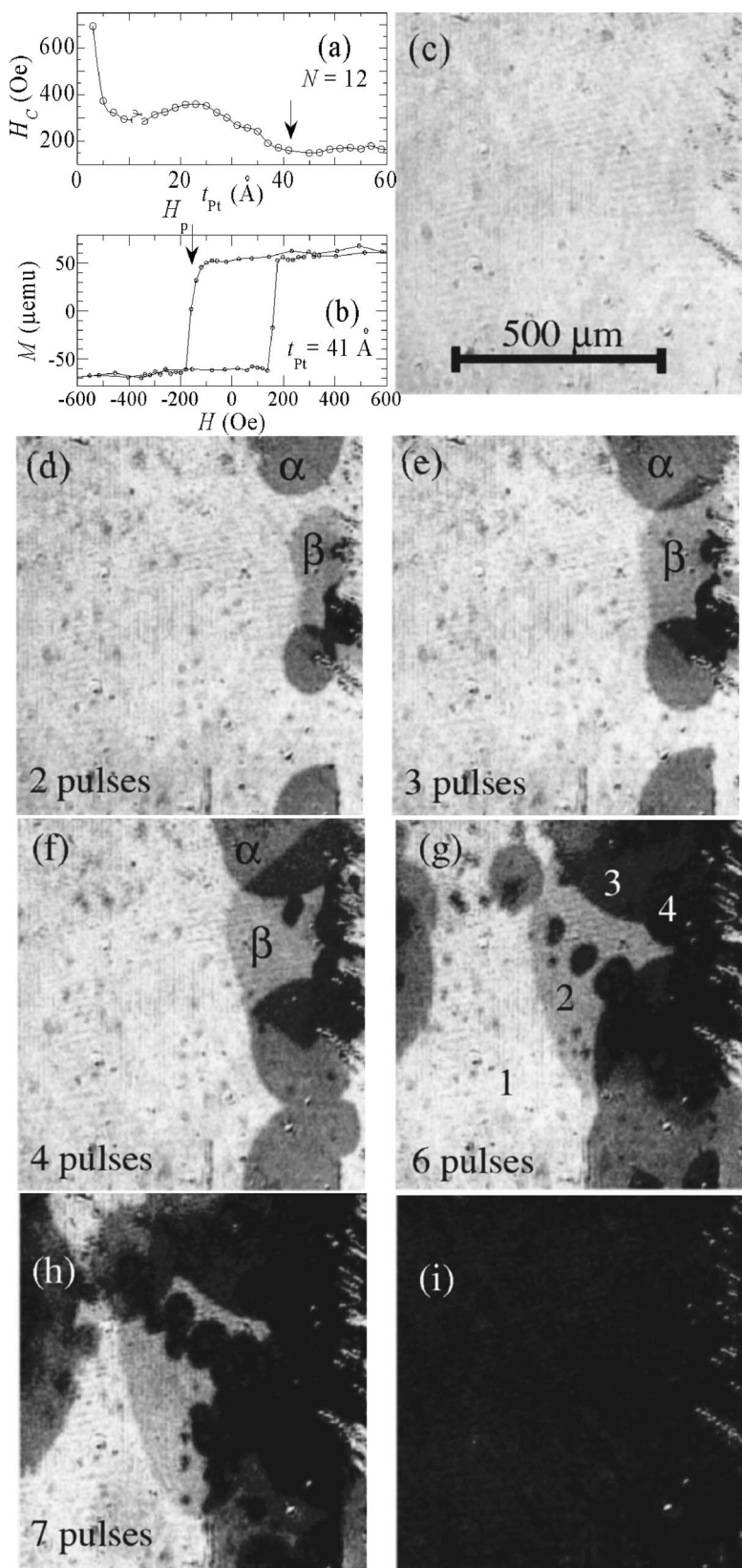


FIG. 4. (a) Room-temperature coercivity for  $[\text{Co}(4 \text{ \AA})/\text{Pt}(t_{Pt})]_N$  multilayers with repetition  $N = 12$ . (b) Hysteresis loop for sample with  $N=12$ ,  $t_{Pt}=41 \text{ \AA}$ . (c)–(h) Kerr microscopy images of  $[\text{Co}(4 \text{ \AA})/\text{Pt}(41 \text{ \AA})]_{12}$  multilayer recorded between repetitive field pulses at  $H_p$  indicated in (b). The corresponding number of field pulses is indicated in each image. The two regions labeled  $\alpha$  and  $\beta$  indicate the evolution of two overlapping domains. (i) Kerr image of  $[\text{Co}(4 \text{ \AA})/\text{Pt}(41 \text{ \AA})]_{12}$  multilayer after being saturated opposite to the initial magnetization.

structure is achieved. The first evidence of layer-by-layer switching in the  $N=5$  multilayer series was observed for  $t_{Pt} = 33 \text{ \AA}$ .

Figure 3 shows the response of similar weakly coupled Co layers ( $t_{Pt}=41 \text{ \AA}$ ) with  $N=8$ . The thickness of the Co/Pt

multilayers, plus the Pt cap layer, is  $390 \text{ \AA}$ —which is larger than the skin depth of the probing laser radiation. Thus, the rotation of the polarization axis of the reflected light recorded in the Kerr images is influenced only by the magnetic state of the top several layers of the multilayers that lie

within the penetration depth of the probe light. Once again, as the field pulses  $H_p$  were applied, the lowest coercivity region begins to switch and grow while, depending on the local coercivity, regions of the other weakly coupled layers sequentially reverse. In Fig. 3(e), four distinct shades (1–4) are evident, revealing the four local magnetic states with different numbers of Co layers reversed. As more field pulses were applied, these domains are observed to grow as their magnetization aligns with the field. Eventually, the stable state of the entire multilayer structure is reached when the magnetization of all domains reverses completely by, and lies parallel to, a large external magnetic field, leading to the uniform black images with a single *down* domain [Fig. 3(g)].

The Kerr images in Figs. 2(e) and 3(e) show that the shapes of the domain boundaries in each sample have certain similarities. For the most part, in each case, the boundary of Domain 4 follows that of Domain 3, which in turn mimics that of Domain 2. While one possible reason for the similar domain patterns is the correlated magnetic switching of the Co layers due to the interlayer coupling; below, we discuss why this is unlikely. Because the RKKY-type interlayer exchange coupling between Co layers becomes negligible at  $t_{\text{Pt}}=41 \text{ \AA}$ , the primary coupling is from the dipole interaction. However, since the separation between adjacent domain walls in Figs. 2 and 3 ranges from about  $50 \mu\text{m}$  to over  $200 \mu\text{m}$ , the correlation arising from the dipole interaction between the Co layers is also negligible. We believe that the observed similarity in domain shapes is likely due to the fact that the Co layers in the multilayer share the same domain nucleation sites, e.g., defects. Since these layers have undergone the same fabrication process and field history, the domain walls in individual Co layers would tend to move along similar paths, resulting in comparable domain shapes, even in the absence of dipole interaction between the Co layers.

The influence of dipole interactions on magnetic switching was evident in a study by Wiebel *et al.*<sup>15</sup> using two stacks of strongly coupled Co/Pt layers sandwiching a  $40 \text{ \AA}$  thick Pt layer. This sample is effectively a trilayer system with two ferromagnetic Co/Pt stacks, each of which behaves as a single ferromagnet. The white decoration ring observed between the dark and the gray regions is a result of the dipole interaction between the two Co/Pt stacks near the domain boundary of the hard stack. The decoration ring is no more than  $3 \mu\text{m}$  wide, which is much smaller when compared to the domain-wall spacing ( $50\text{--}200 \mu\text{m}$ ) as shown in Figs. 2 and 3 for the Co/Pt multilayers of this study.

We note that although the Pt layer thicknesses are essentially the same ( $40 \text{ \AA}$  and  $41 \text{ \AA}$ , respectively) between the Co/Pt stacks in Ref. 15 and in our Co/Pt multilayers, the interlayer interaction has a distinctively different effect on the domain pattern during magnetic reversal. This difference is because the two Co/Pt stacks used in Ref. 15 have equivalent Co thicknesses of  $24 \text{ \AA}$  and  $12 \text{ \AA}$ , respectively, and are thus stronger ferromagnets than the  $4 \text{ \AA}$  thick Co layers in our samples. The strong ferromagnets in Ref. 15 produce large stray fields, resulting in strong dipole interaction between the two Co/Pt stacks to correlate their magnetic switching. On the other hand, the  $4 \text{ \AA}$  Co layers in our samples, each separated by  $41 \text{ \AA}$  Pt layers, are so thin that the stray field (consequently, the dipole interaction) is not

large enough to produce a noticeable correlation between the Co layers during magnetic switching.

While some Kerr images, such as Figs. 2(e) and 3(e) show similar domain boundary shapes, other images reveal neighboring domain walls with very different contours. For example, in moving from Figs. 3(e) and 3(f), the boundary of Domain 3 remains smooth, while Domain 4 develops two peninsular-shaped dark regions indicated by the white arrows in Fig. 3(f). Although the Co layers in each multilayer experienced the same fabrication process and field history, some structural and magnetic variations still exist in these layers. Without the dipole interaction to correlate the Co layers, these variations can lead to different domain shapes in some regions of the Co layers during the magnetic switching process. Such dissimilarity in domain contours is consistent with our previous assertion of uncorrelated magnetic switching.

The uncorrelated magnetic reversal is more clearly evident in Fig. 4 for Co/Pt multilayers with  $N=12$  and  $t_{\text{Pt}}=41 \text{ \AA}$ . Similar to Figs. 2 and 3, four different shades of domains are observed, as indicated in Fig. 4(g). One interesting feature is the evolution of two domains labeled  $\alpha$  and  $\beta$  in the upper right part of Figs. 4(d)–4(f). In Fig. 4(d), domains  $\alpha$  and  $\beta$  are separate. As more field pulses are applied to the multilayer, domains  $\alpha$  and  $\beta$  expand, meet, and start to overlap as shown in Fig. 4(e). The overlap region between domains  $\alpha$  and  $\beta$  grows in Fig. 4(f). It is clear that in this case overlapped domains  $\alpha$  and  $\beta$  retain their original shapes with each domain behaving as if the other one does not exist. The overlapping of the two domains is analogous to putting two sunshades atop each other to make a darker sunshade. If the dipole interaction between the Co layers is not negligible, the two domains will influence each other and show a correlation between them, resulting in domain shape distortion. This is not the case in Fig. 4. To the contrary, evidence in Figs. 4(d)–4(f) suggests that the dipole interaction between the Co layers is so weak that the magnetic switching of one Co layer does not influence that of the other Co layers. The magnetization of one domain associated with some reversed Co layer(s) has no effect on the overlapping domain from other Co layer(s). It is also noticed that there are some scratches near the right edge of the images in Fig. 4. These scratches only influence the domain nucleation stage of the magnetic reversal. As the domain walls move tens of micrometers away from the scratches, these defects have no significant influence on either the domain-wall motion or the interlayer coupling.

It is evident that the magnetization of the perpendicularly magnetized films has been determined with relatively high spatial resolution. With an external field applied opposite to the magnetization of the fully magnetized multilayers, the formation of small domains of reversed magnetization is observed. The hysteresis loops [Figs. 1(b), 2(b), 3(b), and 4(b)] of the four samples in this study display the magnetization reversal with abrupt switching for the entire samples; while the Kerr images reveal the microscopic layer-by-layer magnetization reversal of Co layers in the Kerr images in Figs. 2–4. In addition, Kerr imaging can also distinguish the difference between magnetic switching within the same series, e.g.,  $N=5$ , between  $t_{\text{Pt}}=11 \text{ \AA}$  (Fig. 1), and  $t_{\text{Pt}}=41 \text{ \AA}$  (Fig. 2), which is not evident in the hysteresis loops.

#### IV. CONCLUSION

In summary, a sequence of short pulses of externally applied magnetic fields are used to reverse the magnetization of  $[\text{Co}(4 \text{ \AA})/\text{Pt}(t_{\text{Pt}})]_N$  multilayers with perpendicular magnetization. Monitored by magneto-optical Kerr imaging, the whole multilayer is observed to switch as a single ferromag-

net for small values of Pt layer thickness when the Co layers exhibit strong coupling. As the Co layers become weakly coupled at a large Pt layer thickness, the Co layers switch separately and details of the layer-by-layer reversal are revealed through the appearance of magnetic domains with distinct shades for Co layers, enriching our understanding of the magnetic reversal mechanism of Co/Pt multilayers.

- 
- <sup>1</sup>A. Moser, K. Takano, D. T. Margulies, M. Albrecht, Y. Sonobe, Y. Ikeda, S. H. Sun, and E. E. Fullerton, *J. Phys. D* **35**, R157 (2002).
- <sup>2</sup>P. Grünberg, R. Schreiber, Y. Pang, M. B. Brodsky, and H. Sower, *Phys. Rev. Lett.* **57**, 2442 (1986).
- <sup>3</sup>M. N. Baibich, J. M. Broto, A. Fert, F. Nguyen Van Dau, F. Petroff, P. Eitenne, G. Creuzet, A. Friederich, and J. Chazelas, *Phys. Rev. Lett.* **61**, 2472 (1988).
- <sup>4</sup>S. Hashimoto, Y. Ochiai, and K. Aso, *J. Appl. Phys.* **66**, 4909 (1989).
- <sup>5</sup>B. N. Engel, C. D. England, R. A. Van Leeuwen, M. H. Wiedemann, and C. M. Falco, *Phys. Rev. Lett.* **67**, 1910 (1991).
- <sup>6</sup>Z. Celinski and B. Heinrich, *J. Magn. Magn. Mater.* **99**, L25 (1991).
- <sup>7</sup>E. E. Fullerton, D. Stoeffler, K. Ounadjela, B. Heinrich, Z. Celinski, and J. A. C. Bland, *Phys. Rev. B* **51**, 6364 (1995); *ibid.* **51**, 6364 (1995).
- <sup>8</sup>J. W. Knepper and F. Y. Yang, *Phys. Rev. B* **71**, 224403 (2005).
- <sup>9</sup>J. Moritz, F. Garcia, J. C. Toussaint, B. Dieny, and J. P. Nozieres, *Europhys. Lett.* **65**, 123 (2004).
- <sup>10</sup>B. E. Argyle and J. G. McCord, *J. Appl. Phys.* **87**, 6487 (2000).
- <sup>11</sup>B. D. Cullidy, *Introduction to Magnetic Materials* (Addison-Wesley, London, 1972).
- <sup>12</sup>D. J. Griffiths, *Introduction to Electrodynamics*, 3rd Ed. (Prentice-Hall, Upper Saddle River, New Jersey, 1999).
- <sup>13</sup>A. Suna, *J. Appl. Phys.* **59**, 313 (1986).
- <sup>14</sup>H. J. G. Draaisma and W. J. M. de Jonge, *J. Appl. Phys.* **62**, 3318 (1987).
- <sup>15</sup>S. Wiebel, J.-P. Jamet, N. Vernier, A. Mougín, J. Ferré, V. Baltz, B. Rodmacq, and B. Dieny *Appl. Phys. Lett.* **86**, 142502 (2005).